J. Fluid Mech. (1993), *vol.* 255, *pp.* 213–236

Reconsideration of Orlanski's instability theory of frontal waves

By KEITA IGA

Ocean Research Institute, University of Tokyo, Tokyo 164, Japan

(Received 6 October 1992 and in revised form 13 April 1993)

This paper complements the instability theory of frontal waves investigated by Orlanski (1968), and reinterprets the unstable modes obtained. First, the stability of a frontal model is reconsidered by using a matrix method. The major part of Orlanski's (1968) result is verified but some flaws are found in some parameter regions: unstable modes do not exist over the entire *Ri*–*Ro* region. Also, the features of the neutral waves in the one-layer subsystems are studied, in order to determine the instability of the full two-layer system. As a result, the unstable mode called the (B)-mode by Orlanski (1968) and suggested by Sakai (1989) to be Rossby–Kelvin instability caused by a resonance between a Rossby wave and a gravity wave, proves to be a geostrophic unstable mode caused by resonance between a Rossby wave and the Rossby–gravity mixed mode. In addition, some of the analytical conclusions about the stability of this frontal model are explained by the features of the neutral waves in the one-layer subsystem.

1. Introduction

In the classical theory of extratropical cyclones, which originated with the Norwegian school, it was suggested that the warm equatorial airmass and the cold polar airmass form a discontinuous interface, and because of the instability of the frontal surface, disturbances develop there to become extratropical cyclones. The problem of the stability of a simple frontal surface was formulated by Kotschin (1932), Orlanski (1968) and others.

Kotschin (1932) considered the stability of the interface in a situation wherein two incompressible homogeneous fluids with a slight density difference flow in the x_*-direction with a shear of ΔU. The fluids were bounded above and below by two rigid horizontal planes with a gap between them of H (figure 1). Because of mathematical difficulties, he only studied the case in which the wavenumber of the disturbance vanishes (the case in which the scale of the disturbance is very large) and also the condition in which a neutral wave exists which propagates with the mean speed of the basic flow.

Orlanski (1968) investigated the same problem of the stability of the frontal surface comprehensively for various combinations of the parameters by numerical calculation, and obtained the following results. The basic state of this frontal model is characterized by the Richardson number *Ri*, and the wavenumber of the disturbance is expressed by the Rossby number *Ro*, defined in §2, equations (16) and (17). Rayleigh shear instability (R) exists at small *Ri*, Kelvin–Helmholtz instability (H) exists at large *Ro* and small *Ri*, shear instability (R) and geostrophic baroclinic instability (E) simultaneously exist at small *Ro* and $Ri > 2$ (the growth rate of (R) is larger than that of (E)), and finally a combination of geostrophic and Kelvin–Helmholtz instability (B)

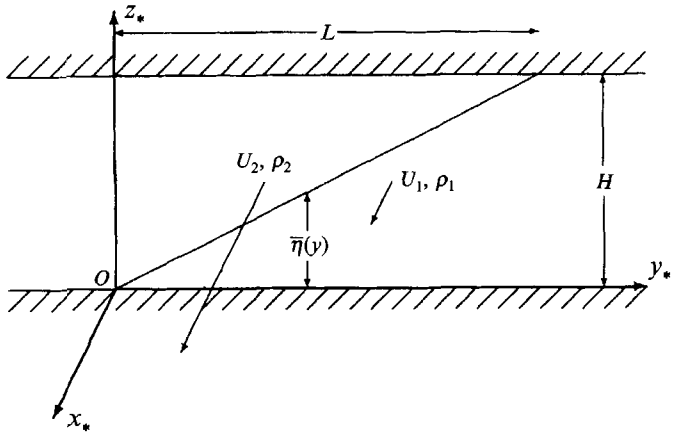

FIGURE 1. Frontal surface model.

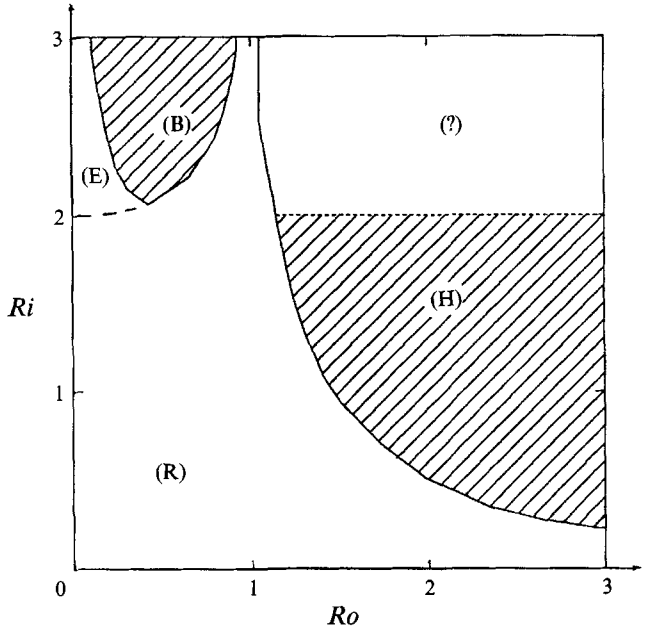

FIGURE 2. Results of Orlanski (1968): the (R)-mode overlies the (E)-mode. The shaded areas indicate complex eigenvalues (non-zero phase speed).

exists at $Ri > 2$ and $Ro < 1$ (but not too small). Unstable waves exist over the entire region of (Ri, Ro)-space and these unstable modes occupy mutually exclusive regions except where the (E)- and (R)-modes simultaneously exist. These results are schematically redrawn in figure 2 (figure 10 in Orlanski's paper).

Incidentally, in the 1960s when Orlanski's paper was written, the classification of the unstable modes was done by investigating the features of the velocity field and of the energy transformation, and the classification by Orlanski (1968) stated above was mainly made on this basis. In the 1980s, however, an idea already familiar in plasma physics that an unstable mode can be understood as a resonance between neutral waves, began to be applied to instability problems in fluid mechanics (e.g. Cairns 1979; Hayashi & Young 1987). The analysis of resonant neutral modes represents an

alternative way of describing the instabilities. Although the consideration of the energy is the basis for identifying the unstable modes, the analysis of neutral waves also will help us to understand the dynamics of the instabilities. Sakai (1989) studied a two-layer problem, and suggested that the (B)-mode in Orlanski (1968) could be a Rossby–Kelvin instability caused by resonance between a Rossby wave and a Kelvin wave, although the problem he investigated was not completely the same as Kotschin's (1932) or Orlanski's (1968), and it was no more than a suggestion.

Thus, the theory for the stability of the frontal surface was started by Kotschin (1932), investigated by Orlanski (1968), and then Sakai (1989) attempted an interpretation from a new point of view, but some problems are still left. The first problem arises from the method which Orlanski (1968) used to search for the eigenvalues. Because of the primitive computing power of that day, he had to use the shooting method, which is a kind of Newton method (trial and error method). The advantage of this method is that an eigenvalue and the corresponding eigenfunction can be obtained in a relatively short time as long as a good initial guess is available for the solution, while the disadvantage is that one cannot be sure of the uniqueness of the solution obtained (e.g. Nakamura 1988). Hence, the question arises whether there might be other overlooked unstable modes. The next problem is that the points in the (*Ri*, *Ro*)-plane for which Orlanski (1968) made the computations were not dense enough. It seems that he completed the diagram shown in figure 2 (his figure 10 is more detailed than this) by inter- and extrapolating the sparse results. Accordingly the question arises whether his diagram is really correct. For example, on the boundaries of (B) and (R) or of (R) and (H), four different modes converge to one point and diverge to four again. This is an unusual branch, since usually only two modes converge to one point. If this diagram is right, such fourfold branching occurs all along these boundaries, which seems unnatural. Furthermore, it is not yet clear how the unstable modes are classified from the new standpoint of the resonance between neutral waves. It would be particularly interesting to know whether Sakai's (1989) suggestion, that the (B)-mode is a Rossby–Kelvin instability, is true.

At present, a front is regarded as the result of the development of an extratropical cyclone rather than the cause of it. Thus, this problem of the stability of a frontal surface has reduced importance as a theory of the development of an extratropical cyclone, which was the main interest of Kotschin (1932) and Orlanski (1968). In the atmosphere and the ocean, however, there are many phenomena in which fluids with different densities form a frontal surface and disturbances develop there. Hence frontal stability retains its importance in meteorology, physical oceanography and geophysical fluid dynamics. Nevertheless, this important and fundamental problem has not been completely investigated. In this paper, we re-examine the results of Orlanski (1968) and classify the unstable modes. First, in §2 this problem is formulated and the equations to be solved are derived. In §3 the computed results are shown and the results of Orlanski (1968) are re-examined. To classify the unstable modes obtained from the standpoint of the resonance between neutral waves, features of the neutral waves in a reduced one-layer fluid are investigated in §4. Using the results in §4, the unstable modes in §3 are explained in §5.

2. Basic equations for the instability problem of the frontal system

2.1. *Basic equations*

As stated in the introduction, the system considered here is that studied by Kotschin (1932) and Orlanski (1968). Two layers of incompressible homogeneous fluid are

bounded above and below by rigid horizontal planes at $z_* = 0$ and $z_* = H$. In the basic state, the fluid of each layer flows uniformly in the x_*-direction (figure 1). The stability of this state is considered hereafter.

The basic equations under the hydrtostatic and Boussinesq approximations are as follows:

$$\left(\frac{\partial}{\partial t_*}+(\boldsymbol{v}_{*j}\cdot\boldsymbol{\nabla}_*)\right)\boldsymbol{v}_{*j} = -f\boldsymbol{k}\times\boldsymbol{v}_{*j}-\frac{1}{\rho}\boldsymbol{\nabla}_* p_{*j}, \tag{1}$$

$$p_{*1}-p_{*2} = \Delta\rho g\eta_*, \tag{2}$$

$$\frac{\partial\eta_*}{\partial t_*} = -\boldsymbol{\nabla}_*\cdot(\eta_*\boldsymbol{v}_{*1}) = \boldsymbol{\nabla}_*\cdot((H-\eta_*)\boldsymbol{v}_{*2}), \tag{3}$$

where $\boldsymbol{\nabla}_* = (\partial/\partial x_*, \partial/\partial y_*)$ is the horizontal gradient operator, $\boldsymbol{k}$ is the vertical unit vector, $\boldsymbol{v}_{*j} = (u_{*j}(x_*, y_*, t_*), v_{*j}(x_*, y_*, t_*))$ is the velocity in the jth layer, $p_{*j}(x_*, y_*, t_*)$ is the pressure in the jth layer (excluding the hydrostatic part), $\eta_*(x_*, y_*, t_*)$ is the height of the interface, f is the Coriolis parameter, H is the depth of the fluids, g is the gravitational acceleration, ρ is the averaged density of the fluids, and $\Delta\rho$ is the density difference between fluids 1 and 2.

In the basic state, fluid of each layer flows homogeneously in the x_*-direction

$$u_{*j} = U_j, \quad v_{*j} = 0, \quad p_{*j} = -\rho f U_j y_*, \quad \eta_* = \frac{\rho f\Delta U}{\Delta\rho g}y_* = \frac{H}{L}y_*, \tag{4}$$

where

$$\Delta U \equiv U_2 - U_1, \quad L \equiv \frac{\Delta\rho g}{\rho f\Delta U}H. \tag{5}$$

We allow this steady state to be perturbed by a small amount. The variables are divided into the basic part and the disturbance part:

$$u_{*j} = U_j + u'_{*j}, \quad v_{*j} = v'_{*j}, \quad p_{*j} = P_j + p'_{*j}, \quad \eta_* = \bar{\eta} + \eta'_*, \tag{6}$$

where

$$P_{*j} \equiv -\rho f U_j y_*, \quad \bar{\eta} \equiv (H/L)y_*. \tag{7}$$

These are substituted in the basic equations, and the terms of higher order are neglected. Assuming a sinusoidal form in the x_*-direction ($u'_{*j}, v'_{*j}, p'_{*j}, \eta'_* \propto \mathrm{e}^{\mathrm{i}k(x_*-c_*t_*)}$), the variables are non-dimensionalized as

$$\left.\begin{aligned} y_* = Ly, \quad u'_{*j} = \tfrac{1}{2}\Delta U u_j, \quad v'_{*j} = \tfrac{1}{2}\Delta U v_j, \\ c_* - \tfrac{1}{2}(U_1+U_2) = \tfrac{1}{2}\Delta U c, \quad \eta'_* = \frac{\rho f\Delta U}{\Delta\rho g}L\eta, \quad p'_{*j} = \rho f\Delta U L p_j. \end{aligned}\right\} \tag{8}$$

Thus, we get the non-dimensional equations

$$\mathrm{i}Ro(c+1)u_1 = -v_1 + 4\mathrm{i}Ri\,Ro\,p_1, \tag{9}$$

$$\mathrm{i}Ro(c+1)v_1 = u_1 + 2\,\mathrm{d}p_1/\mathrm{d}y, \tag{10}$$

$$\mathrm{i}Ro(c-1)u_2 = -v_2 + 4\mathrm{i}Ri\,Ro\,p_2, \tag{11}$$

$$\mathrm{i}Ro(c-1)v_2 = u_2 + 2\,\mathrm{d}p_2/\mathrm{d}y, \tag{12}$$

$$p_1 = p_2 = \eta, \tag{13}$$

$$\mathrm{i}Ro(c+1)\eta = \mathrm{i}Ro\,yu_1 + \frac{1}{2Ri}\frac{\mathrm{d}}{\mathrm{d}y}(yv_1), \tag{14}$$

$$\mathrm{i}Ro(c-1)\eta = -\mathrm{i}Ro(1-y)u_2 - \frac{1}{2Ri}\frac{\mathrm{d}}{\mathrm{d}y}((1-y)v_2). \tag{15}$$

Non-dimensional parameters Ro and Ri are defined as

$$Ro \equiv \frac{k\Delta U}{2f}, \tag{16}$$

$$Ri \equiv \frac{fL}{\Delta U} = \frac{gH}{(\Delta U)^2}\frac{\Delta\rho}{\rho}. \tag{17}$$

2.2. *Boundary conditions*

We can get the boundary conditions at $y = 0$ and 1 by investigating the solutions at $y < 0$ and $y > 1$. The motion of the fluid at $y > 1$ is described by the equations of motion in the x- and y-directions and the equation of non-divergence. Hence, when $y > 1$, the linearized and non-dimensionalized equations for the small disturbances are (9), (10) and

$$2\mathrm{i}Ri\,Ro\,u_1 + \mathrm{d}v_1/\mathrm{d}y = 0. \tag{18}$$

Eliminating u_1 and p_1, we get

$$4Ri^2\,Ro^2\,v_1 - \mathrm{d}^2v_1/\mathrm{d}y^2 = 0. \tag{19}$$

Since the solution that remains finite as $y \to \infty$ is

$$v_1 = A\,\mathrm{e}^{-2Ri\,Ro\,y}, \tag{20}$$

we get

$$\mathrm{d}v_1/\mathrm{d}y = -2Ri\,Ro\,v_1. \tag{21}$$

Substitution of (21) into (18) results in

$$u_1 = -\mathrm{i}v_1. \tag{22}$$

Because of the continuity of p_1 and v_1 (accordingly the continuity of u_1 and v_1), we obtain the following boundary condition:

$$u_1 = -\mathrm{i}v_1 \quad \text{at} \quad y = 1. \tag{23}$$

In a similar way, we get

$$u_2 = \mathrm{i}v_2 \quad \text{at} \quad y = 0. \tag{24}$$

Furthermore,

$$u_1, v_1 \quad \text{regular at} \quad y = 0, \tag{25}$$

$$u_2, v_2 \quad \text{regular at} \quad y = 1, \tag{26}$$

are assumed.

2.3. *Derivation of the eigenvalue problem*

Orlanski (1968) eliminated u_j and v_j, and derived the equations for p_1 and p_2. However, following Sakai (1989), we will derive equations of the form $\boldsymbol{A}\boldsymbol{z} = c\boldsymbol{z}$ in this subsection, because we can then get the eigenvalues c directly.

At first, we obtain the vorticity equations by subtracting $\mathrm{d}/\mathrm{d}y$ of (9) from $2\mathrm{i}Ri\,Ro$ times (10), and $\mathrm{d}/\mathrm{d}y$ of (11) from $2\mathrm{i}Ri/Ro$ times (12),

$$\mathrm{i}Ro(c+1)\,\zeta_1 = D_1, \tag{27}$$

$$\mathrm{i}Ro(c-1)\,\zeta_2 = D_2, \tag{28}$$

where ζ_j and D_j express the vorticity and the divergence in each layer, respectively:

$$\zeta_j \equiv 2\mathrm{i}Ri\,Ro\,v_j - \mathrm{d}u_j/\mathrm{d}y, \tag{29}$$

$$D_j \equiv 2\mathrm{i}Ri\,Ro\,u_j + \mathrm{d}v_j/\mathrm{d}y. \tag{30}$$

Addition of (15) to (14) and subtraction of (15) from (14) gives

$$2\mathrm{i}Ro\, c\eta = \frac{1}{2Ri}(FD_1 - FD_2), \tag{31}$$

$$2\mathrm{i}Ro\, \eta = \frac{1}{2Ri}(FD_1 + FD_2), \tag{32}$$

where FD_j is the divergence of the mass transport in each layer,

$$FD_1 \equiv 2\mathrm{i}Ri\, Ro\, yu_1 + \frac{\mathrm{d}}{\mathrm{d}y}(yv_1), \tag{33}$$

$$FD_2 \equiv 2\mathrm{i}Ri\, Ro(1-y)u_2 + \frac{\mathrm{d}}{\mathrm{d}y}((1-y)v_1). \tag{34}$$

From (31) and (32), we obtain

$$c(FD_1 + FD_2) = FD_1 - FD_2. \tag{35}$$

Also, substitution of (13) into (9)–(11) results in

$$\mathrm{i}Ro\, c(u_1 - u_2) + \mathrm{i}Ro(u_1 + u_2) = -(v_1 - v_2) + 4\mathrm{i}Ri\, Ro\, \eta. \tag{36}$$

Substituting (32) into (36), we get

$$\mathrm{i}Ro\, c(u_1 - u_2) + \mathrm{i}Ro(u_1 + u_2) = yD_1 + (1-y)D_2, \tag{37}$$

where $FD_1 - v_1 = yD_1$ and $FD_2 + v_2 = (1-y)D_2$ are used. Therefore, the equations for the eigenvalue problem are as follows:

$$\mathrm{i}Ro\, c\zeta_1 = -\mathrm{i}Ro\, \zeta_1 + D_1, \tag{38}$$

$$\mathrm{i}Ro\, c\zeta_2 = \mathrm{i}Ro\, \zeta_2 + D_2, \tag{39}$$

$$c(FD_1 + FD_2) = FD_1 - FD_2, \tag{40}$$

$$\mathrm{i}Ro\, c(u_1 - u_2) = -\mathrm{i}Ro(u_1 + u_2) + yD_1 + (1-y)D_2. \tag{41}$$

3. Numerical solutions

The numerical results, which are obtained by solving the eigenvalue problem (38)–(41) under the boundary conditions (23)–(26) will be shown in this section. The numerical method is described in detail in Appendix A.

Figure 3 shows the isolines of $|c_i|$ for the first and the second unstable modes (unstable modes with the largest and the second largest growth rates, for given values of Ri and Ro) in the (Ri, Ro)-plane. The region $0 < Ro < 3$ and $0 < Ri < 3$ is shown for the first unstable mode, but only $0 < Ro < 1$ and $2 < Ri < 3$ for the second unstable mode. Figures 4, 5 and 6 show the values of c_r and $|c_i|$ as functions of Ro for the cases $Ri = 1.0$, 2.1 and 3.0, respectively.

By comparing figure 3 with figure 2 (the result of Orlanski 1968), the following facts are made clear. First, the curve of $c = 0$ can be recognized as the boundary of the (R)-region in figure 3 (partly as the boundary of the (E)-region). This curve starts at $(Ro, Ri) = (0, 2)$, having a singularity at $Ro = 1$ and approaching $Ri \sim 2Ro^{-2}$ asymptotically as Ro grows; this agrees with the numerical results by Orlanski (1968)

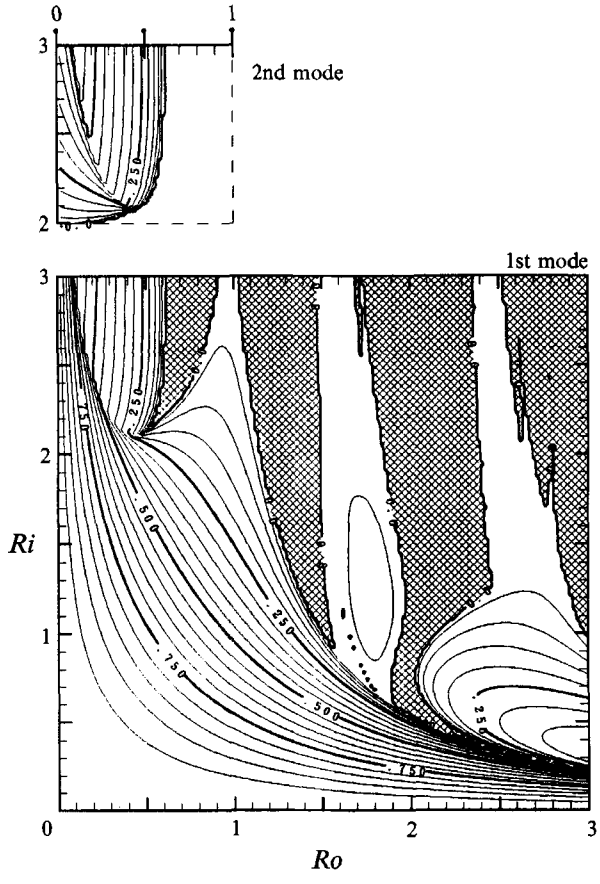

FIGURE 3. The isolines of $|c_i|$ for the first mode as a function of Ri and Ro. The contour intervals are 0.05. Hatched areas indicate the regions where there is no unstable mode (where $|c_i|$ of the first mode is zero). Refer to figure 2 for the location of the (R)-, (E)-, (B)- and (H)-modes. The isolines of $|c_i|$ for the second mode are shown only in the region $0 < Ro < 1.0$ and $2.0 < Ri < 3.0$.

and the analytical results by Kotschin (1932). The transition from the boundary of the (E)-region to that of the (R)-region occurs at $Ri \sim 2.10, Ro \sim 0.48$, although Orlanski (1968) gave the values as $Ri \sim 2.05, Ro \sim 0.35$.

The features of the (R)- and (E)-modes are almost the same as the results by Orlanski (1968) that are sketched in figure 2. For the (R)-mode (see figure 3), the value of $|c_i|$ approaches 1 as either Ri or Ro decreases. Except in the region of $Ro \sim 1$ and $Ri > 1$, $|c_i|$ diminishes in value as either Ri or Ro increases. The (R)-mode extends as far as the curve of $c = 0$ mentioned above (except for the region of $Ri > 2$ and small Ro where this mode extends beyond this curve). The (E)-mode is located in the region of $Ri > 2$ and small Ro, and lies underneath the (R)-mode (compare figures 4 and 5). Figure 5 shows that the values of c are pure imaginary both for the (R)-mode and for the (E)-mode.

Where the (E)- and (R)-modes simultaneously exist, they approach each other as Ro grows, to coalesce into a new mode (B) (see figure 6). The value of c for the (B)-mode is complex, and as Ro grows further, the value of $|c_i|$ decreases, finally to vanish where this (B)-mode ends. These features of the (B)-mode agree with the results by Orlanski (1968), apart from a slight discrepancy. He thought that $|c_r|$ vanished together with $|c_i|$,

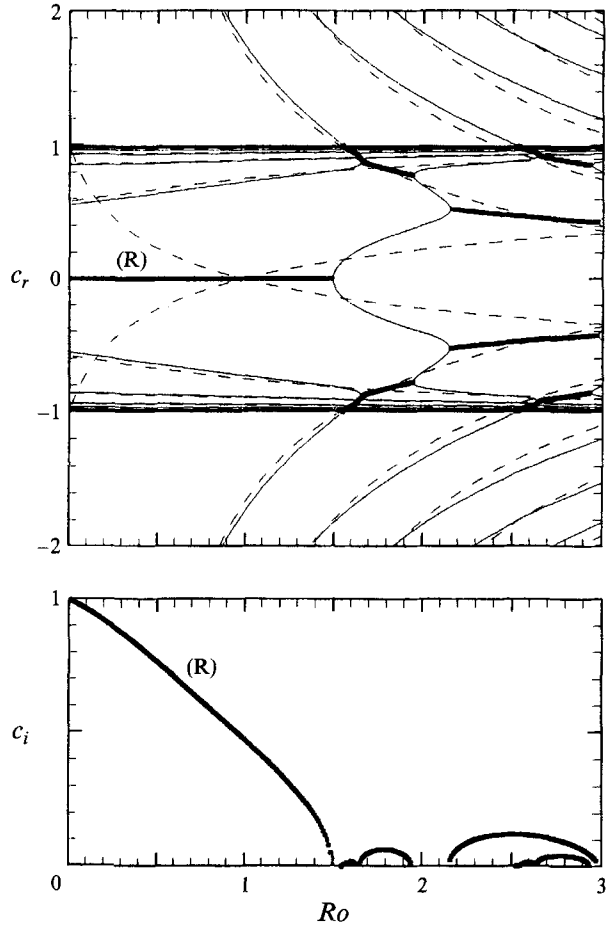

FIGURE 4. The values of c_r and $|c_i|$ as functions of Ro at $Ri = 1.0$. Unstable modes are shown by thick lines. Instability occurs where two dispersion curves intersect. Dashed lines indicate the Doppler-shifted dispersion curves of the one-layer problem for the same Ri (see §5).

and hence the (B)-mode extended as far as the curve of $c = 0$ to bound on the (R)-mode, whereas $|c_r|$ does not vanish in reality as shown by figure 6, and consequently there is a gap between the (B)- and (R)-regions where there is no unstable mode (see figure 3).

The behaviour of the unstable modes in the region of (H) is quite different from the results by Orlanski (1968). Although he thought that a single unstable mode with characteristics of Kelvin–Helmholtz instability spread over this region, figure 3 shows that this region is not so simple. There exist several unstable modes; some of them are overlapping and some of them have a gap with the neighbouring mode. Thus, there is no unstable mode in some regions, and there is more than one unstable mode in other regions.

In this way, the early results of Orlanski (1968) in the regions of (R), (E) and part of (B), are verified by this study, but the regions of (H) and part of (B) were not correctly described by him. In particular, his result that unstable waves exist in the entire (Ri, Ro)-plane is incorrect.

The dispersion relations of figures 4, 5 and 6 show that instability occurs where two dispersion curves intersect. Hence, the unstable modes can be interpreted as resonances

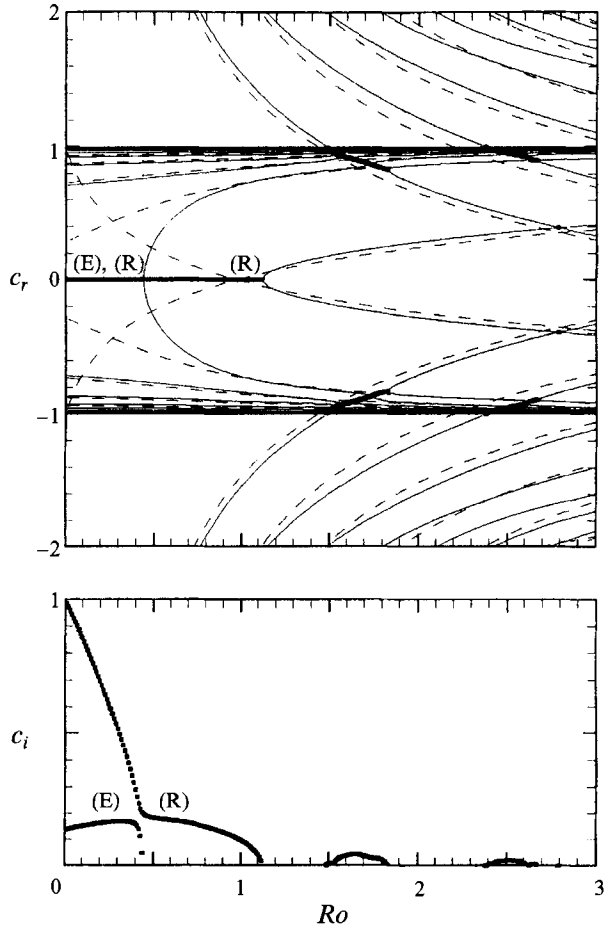

FIGURE 5. Same as figure 4, but for $Ri = 2.1$. Unstable mode (E) appears at $Ro < 0.45$.

between neutral waves, as done by Satomura (1981), Hayashi & Young (1987), Sakai (1989) and others. There will be a consideration of which waves resonate to cause the unstable modes in later sections.

Another conspicuous feature of figures 4, 5 and 6 is that there are many dispersion curves bunched around $c = \pm 1$. These bundles of dispersion curves will be also explained in later sections.

4. Waves in a one-layer fluid

According to Sakai (1989), the physical mechanism of an unstable mode in the two-layer problem can be understood as a resonance between neutral waves in the reduced one-layer subsystems. To identify the waves which resonate to cause the unstable modes found in the previous section, we will consider the one-layer subsystem in this section, by making the depth of the upper (or lower) layer infinite. If we look at this subsystem moving with the homogeneous basic flow in the x_*-direction, it is equivalent to a flow over a slope followed by a flat bottom. (The fluid is bounded by a rigid plane over the flat bottom. See figure 7.) For this one-layer system, one can easily imagine

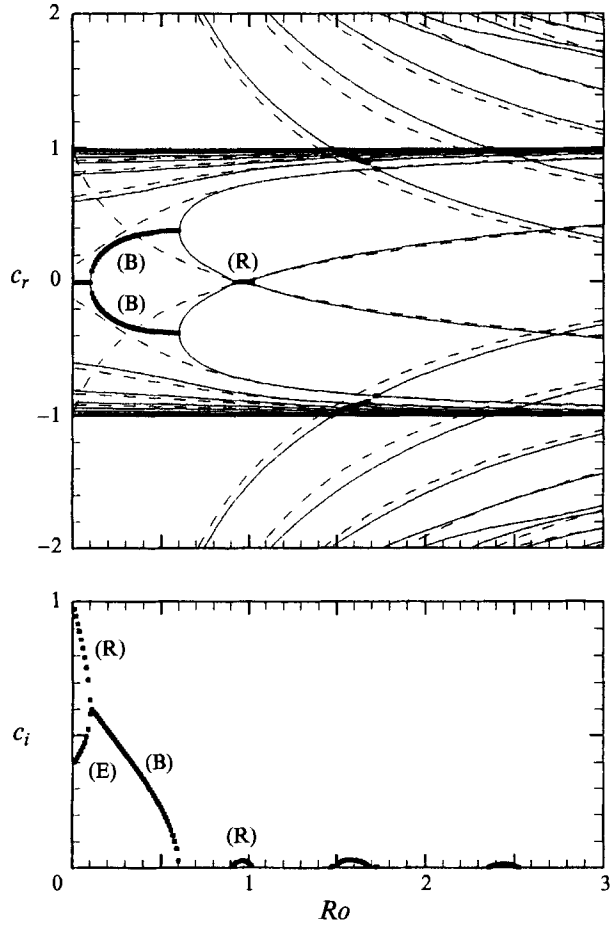

FIGURE 6. Same as figure 4, but for $Ri = 3.0$. Unstable modes (R) and (E) simultaneously exist at $Ro < 0.1$, and they coalesce into a new mode (B) at $0.1 < Ro < 0.6$. The unstable mode located around $Ro = 1.0$ is also an (R)-mode.

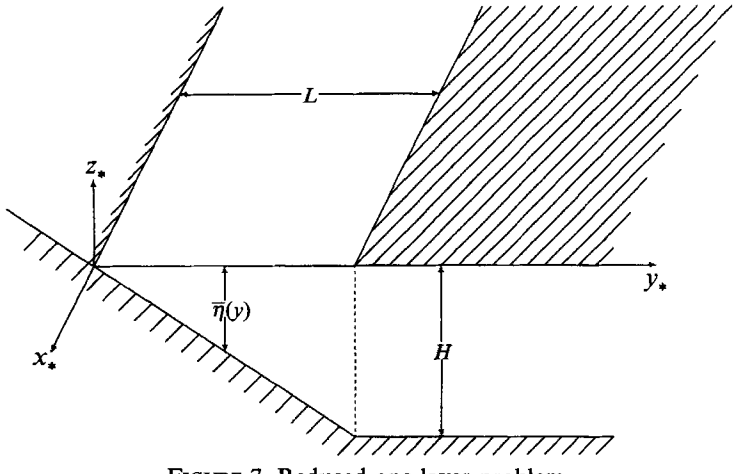

FIGURE 7. Reduced one-layer problem.

that there exist inertial gravity waves and topographical Rossby waves. The unstable modes in the two-layer model can be understood as resonances between these inertial gravity waves and Rossby waves, whose features are relatively well known.

In fact, a very similar problem is that in physical oceanography of 'edge waves' which are trapped on a gently sloping beach or continental shelf. Since the situation we are considering now is, of course, unnatural as a model for a sloping shelf, exactly the same problem has not been solved yet. For example, in Reid's (1958) model, the sloping shelf is semi-infinite, and in those of Robinson (1964) and Mysak (1968), the sloping shelf has a finite width that drops off vertically into deep water of constant depth. The problem we are considering now is governed by the same basic equations in the internal region, but has different boundary conditions from these previous studies.

4.1. *Basic equations*

The non-dimensional basic equations for each Fourier component at $0 < y < 1$ are as follows:

$$\mathrm{i}Ro\,cu = -v + 4\mathrm{i}Ri\,Ro\,\eta, \tag{42}$$

$$\mathrm{i}Ro\,cv = u + 2\,\mathrm{d}\eta/\mathrm{d}y, \tag{43}$$

$$\mathrm{i}Ro\,c\eta = \mathrm{i}Ro\,yu + \frac{1}{2Ri}\frac{\mathrm{d}}{\mathrm{d}y}(yu). \tag{44}$$

The boundary conditions are the same as those for the two-layer problem:

$$u = -\mathrm{i}v \quad \text{at} \quad y = 1, \tag{45}$$

$$u \text{ and } v \text{ regular at } y = 0, \tag{46}$$

expressed in terms of u and v (see (23) and (25) in §2), and

$$\mathrm{d}\eta/\mathrm{d}y = -2Ri\,Ro\,\eta \quad \text{at} \quad y = 1, \tag{47}$$

$$\eta \text{ and } \mathrm{d}\eta/\mathrm{d}y \text{ regular at } y = 0, \tag{48}$$

expressed in terms of η and $\mathrm{d}\eta/\mathrm{d}y$ ((3.13), (3.16) in Orlanski 1968).

Eliminating u and v, this problem reduces to an equation for one variable, η. Equations (42) and (43) allow u and v to be expressed as linear functions of η and $\mathrm{d}\eta/\mathrm{d}y$,

$$u = \frac{4Ri\,Ro^2\,c\eta + 2\,\mathrm{d}\eta/\mathrm{d}y}{Ro^2\,c^2 - 1}, \tag{49}$$

$$v = -\mathrm{i}\frac{4Ri\,Ro\,\eta + 2Ro\,c\,\mathrm{d}\eta/\mathrm{d}y}{Ro^2\,c^2 - 1}. \tag{50}$$

Substitution of (49) and (50) in (44) results in an equation for η,

$$\frac{\mathrm{d}}{\mathrm{d}y}\left(y\frac{\mathrm{d}\eta}{\mathrm{d}y}\right) + [Ri(Ro^2\,c^2 - 1 + 2/c) - 4Ri^2\,Ro^2\,y]\,\eta = 0. \tag{51}$$

4.2. *Eigenvalues and eigenfunctions*

Solving (51) under the boundary conditions (47) and (48), is a problem of Sturm–Liouville type. Hence, it has an infinite series of eigenvalues $\lambda_n (n = 0, 1, 2, \ldots)$,

$$Ri(Ro^2\,c_n^2 - 1 + 2/c_n) = \lambda_n(Ri\,Ro). \tag{52}$$

Since this is a cubic equation for c_n, there exist three c_n for each n.

Let us see what kind of wave each mode corresponds to. Assume that each wave satisfies either $Ro\,c_n \ll 1$ or $Ro\,c_n \gg 1$; the modes are split clearly into waves of low frequency and high frequency. For the modes with $Ro\,c_n \ll 1$, by neglecting $Ro^2 c_n^2$, we obtain

$$c_n \sim \frac{2}{\lambda_n(Ri\,Ro)/Ri+1}. \tag{53}$$

For $Ri\,Ro \gg 1$, since $\lambda_n(Ri\,Ro)$ is almost equal to $4Ri\,Ro(n+\frac{1}{2})$ (this can be obtained by considering the behaviour of Laguerre functions (Appendix B), the concrete form of η_n being given in (60)), the relation (53) becomes

$$c_n \sim \frac{2}{4Ro(n+\frac{1}{2})+1}, \tag{54}$$

and this corresponds to almost geostrophic-balanced Rossby modes. On the other hand, for the modes with $Ro\,c_n \gg 1$, by neglecting $2Ri/c_n$, we obtain

$$c_n \sim \pm\frac{1}{Ro}\left(1+\frac{\lambda_n(Ri\,Ro)}{Ri}\right)^{\frac{1}{2}}. \tag{55}$$

For $Ri\,Ro \gg 1$, (55) becomes

$$c_n \sim \pm\frac{1}{Ro}(1+4Ro(n+\tfrac{1}{2}))^{\frac{1}{2}}, \tag{56}$$

and these correspond to Poincaré modes.

The eigenfunction η_n corresponding to the eigenvalue λ_n can be obtained as follows. Substitution of $z \equiv 4Ri\,Ro\,y$ and $\eta_n \equiv \mathrm{e}^{-2Ri\,Ro\,y}\xi_n = \mathrm{e}^{-\frac{1}{2}z}\xi_n$ into (51) results in

$$z\frac{\mathrm{d}^2\xi_n}{\mathrm{d}z^2}+(1-z)\frac{\mathrm{d}\xi}{\mathrm{d}z}+\left[\frac{\lambda_n}{4Ri\,Ro}-\frac{1}{2}\right]\xi_n = 0, \tag{57}$$

and this ξ_n satisfies the boundary condition,

$$\frac{\mathrm{d}\xi_n}{\mathrm{d}z} = 0 \quad \text{at} \quad z = 4Ri\,Ro. \tag{58}$$

Equation (57) is Laguerre's differential equation, and the solutions which are regular at $z = 0$ are expressed by Laguerre functions (Appendix B). Thus, we obtain

$$\begin{aligned}\xi_n &= L^{(0)}_{\frac{\lambda_n}{4Ri\,Ro}-\frac{1}{2}}(z)\\ &= L^{(0)}_{\frac{\lambda_n}{4Ri\,Ro}-\frac{1}{2}}(4Ri\,Ro\,y),\end{aligned} \tag{59}$$

or

$$\eta_n = \mathrm{e}^{-2Ri\,Ro\,y}L^{(0)}_{\frac{\lambda_n}{4Ri\,Ro}-\frac{1}{2}}(4Ri\,Ro\,y). \tag{60}$$

4.3. *Special cases*

We cannot obtain the values of λ_n analytically in general, but λ_0 for the fundamental mode can be obtained. When $\nu = 0$, Laguerre function $L_\nu^{(0)}(z)$ becomes $L_0^{(0)}(z) = 1$, which clearly satisfies the boundary condition $\mathrm{d}L_0^{(0)}(z)/\mathrm{d}z = 0$ at $z = 4Ri\,Ro$. Hence,

$\eta = e^{-\frac{1}{2}z}$ is one of the eigenfunctions. Moreover, when $\nu < 0$, $L_\nu^{(0)}(z)$ never satisfies $dL_\nu^{(0)}(z)/dz = 0$ (Appendix B), and thus $L_0^{(0)}(z) = 1$ is the eigenfunction for the smallest eigenvalue. Consequently, we obtain the zeroth (fundamental) eigenvalue,

$$\lambda_0/4Ri\,Ro - \tfrac{1}{2} = 0,$$

or

$$\lambda_0 = 2Ri\,Ro, \tag{61}$$

and the fundamental eigenfunction,

$$\eta_0 = e^{-2Ri\,Ro\,y}. \tag{62}$$

We can also obtain c_0,

$$Ri\left(Ro^2 c_0^2 - 1 + \frac{2}{c_0}\right) = 2Ri\,Ro,$$

or

$$c_0 = \frac{-1 \pm (1+8Ro)^{\frac{1}{2}}}{2Ro}. \tag{63}$$

(The other solution, $c_0 = 1/Ro$, is not acceptable, because u and v cannot be determined for this c_0.) In particular, whatever the value of Ri is,

$$c_0 = 1 \text{ or } -2 \quad \text{at} \quad Ro = 1. \tag{64}$$

The velocity field of the fundamental mode can be obtained from (49) and (50):

$$u_0 = \frac{4Ri\,Ro}{Ro\,c_0 + 1}\eta_0 = \frac{4Ri\,Ro}{Ro\,c_0 + 1}e^{-2Ri\,Ro\,y}, \tag{65}$$

$$v_0 = i\frac{4Ri\,Ro}{Ro\,c_0 + 1}\eta_0 = i\frac{4Ri\,Ro}{Ro\,c_0 + 1}e^{-2Ri\,Ro\,y}. \tag{66}$$

The orbit of each fluid particle is circular, and both divergence and vorticity vanish for this velocity field.

The case of $Ro \to 0$ is investigated as another special case. Here, (51) and the boundary condition (47) becomes

$$\frac{d}{dy}\left(y\frac{d\eta}{dy}\right) + \left(Ri\,Ro^2 c^2 - Ri + \frac{2Ri}{c}\right)\eta = 0, \tag{67}$$

$$\frac{d\eta}{dy} = 0 \quad \text{at} \quad y = 1. \tag{68}$$

Substitution of $2\{(Ri\,Ro^2 c^2 - Ri + 2Ri/c)\,y\}^{\frac{1}{2}} \equiv z$ into (67) and (68) results in

$$\frac{d^2\eta}{dz^2} + \frac{1}{z}\frac{d\eta}{dz} + \eta = 0, \tag{69}$$

$$\frac{d\eta}{dz} = 0 \quad \text{at} \quad z = 2\left(Ri\,Ro^2 c^2 - Ri + \frac{2Ri}{c}\right)^{\frac{1}{2}}. \tag{70}$$

From (69) the regular solution at $z = 0$ is expressed by a Bessel function of zeroth order,

$$\eta = J_0(z)$$
$$= J_0(2\{(Ri\,Ro^2 c^2 - Ri + 2Ri/c)\,y\}^{\frac{1}{2}}), \tag{71}$$

and from the boundary condition (70),

$$2(Ri\,Ro^2 c_n^2 - Ri + 2Ri/c_n)^{\frac{1}{2}} = 2\lambda_n^{\frac{1}{2}} = j_{n+1,1} \tag{72}$$

is obtained, where $j_{n+1,1}$ is the $(n+1)$th zero of $\mathrm{d}J_0(z)/\mathrm{d}z = -J_1(z)$. By putting $Ro\,c_n \ll 1$, we can obtain c_n for the Rossby modes,

$$c_n = \frac{2}{j_{n+1,1}^2/4Ri + 1}. \tag{73}$$

For the higher modes, the $j_{n+1,1}$ are approximated as

$$j_{n+1,1} \sim (n+\tfrac{9}{4})\pi, \tag{74}$$

hence, the c_n are estimated as

$$c_n \sim \frac{2}{(n+\frac{9}{4})^2\pi^2/4Ri + 1}. \tag{75}$$

Ri_n, the value of Ri for which c_n equals 1 is obtained as follows:

$$Ri_n \sim \tfrac{1}{4}(n+\tfrac{9}{4})^2\pi^2. \tag{76}$$

4.4. *Numerical solutions*

The numerical results obtained by solving the eigenvalue problem (42)–(44) under the boundary conditions (45) and (46) will be given in this subsection. The numerical method is described in detail in Appendix A. Figure 8 shows the dispersion relation (Ro–(ω_*/f)) for the case $Ri = 3.0$. For different value of Ri the qualitative characteristics are the same as in this case, although the curves are shifted quantitatively. As is expected from the earlier subsections, there are three types of wave modes in this system:

Rossby waves	(M_0)	R_1	R_2	$R_3\ldots,$
inertial gravity waves in the positive direction	(M_0)	G_1^+	G_2^+	$G_3^+\ldots,$
inertial gravity waves in the negative direction	G_0^-	G_1^-	G_2^-	$G_3^-\ldots.$

These three types of waves were also found in the models of Reid (1958) and Mysak (1968).

The mode M_0 cannot be easily classified, because it is a mixture of a Rossby mode and a Poincaré mode. When the wavenumber is small, this mode behaves like a Rossby wave, but when the wavenumber is large, it behaves like an inertial gravity wave. This mixed mode M_0 was also found in Reid's (1958) model, although not in Mysak's (1968). Furthermore, this mixed mode, in spite of the difference of the boundary conditions, has precisely the same dispersion relation and structure in the model considered now and in Reid's (1958) model, because this solution exactly satisfies both boundary conditions. Since this mode is the fundamental (zeroth) one, the features are known analytically as was seen before. In particular, for this M_0 mode, $Ro\,c$ exactly equals 1 ($\omega_* = f$ in dimensional units) at $Ro = 1$, whatever the value of Ri. For a small wavenumber, the M_0 mode is like a Rossby wave, and for a large wavenumber it is like an inertial gravity wave as mentioned above, whose transition point is around $Ro = 1$, depending on which is greater, the frequency of the wave or the Coriolis parameter.

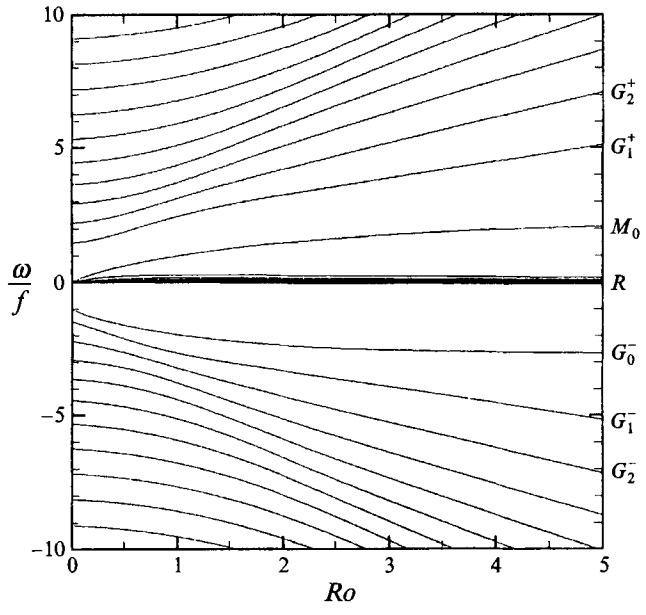

FIGURE 8. $Ro\,c = \omega_*/f$ as a function of Ro at $Ri = 3.0$. The modes are categorized into three types: inertial gravity waves with large frequencies which propagate in the positive (G_n^+) and in the negative (G_n^-) directions, and Rossby waves with small frequencies propagating in the positive direction (R_n). The Rossby waves are so close together that individual R_n are not shown. The curves of G_n with $n > 2$ are not labelled.

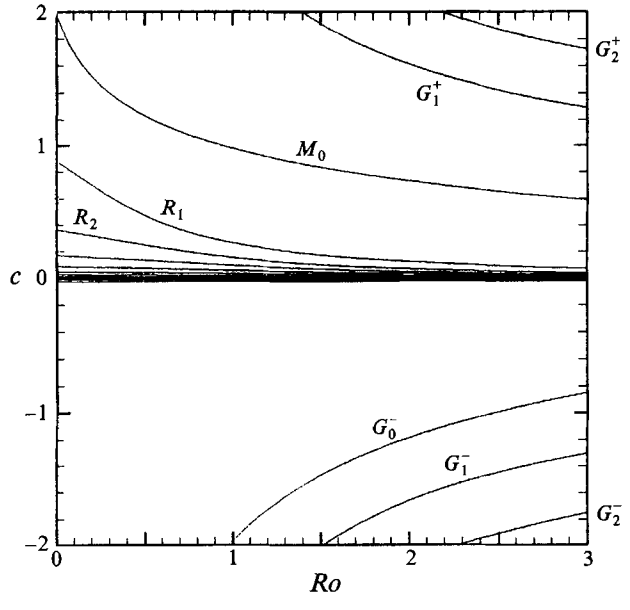

FIGURE 9. c as a function of Ro for $Ri = 3.0$.

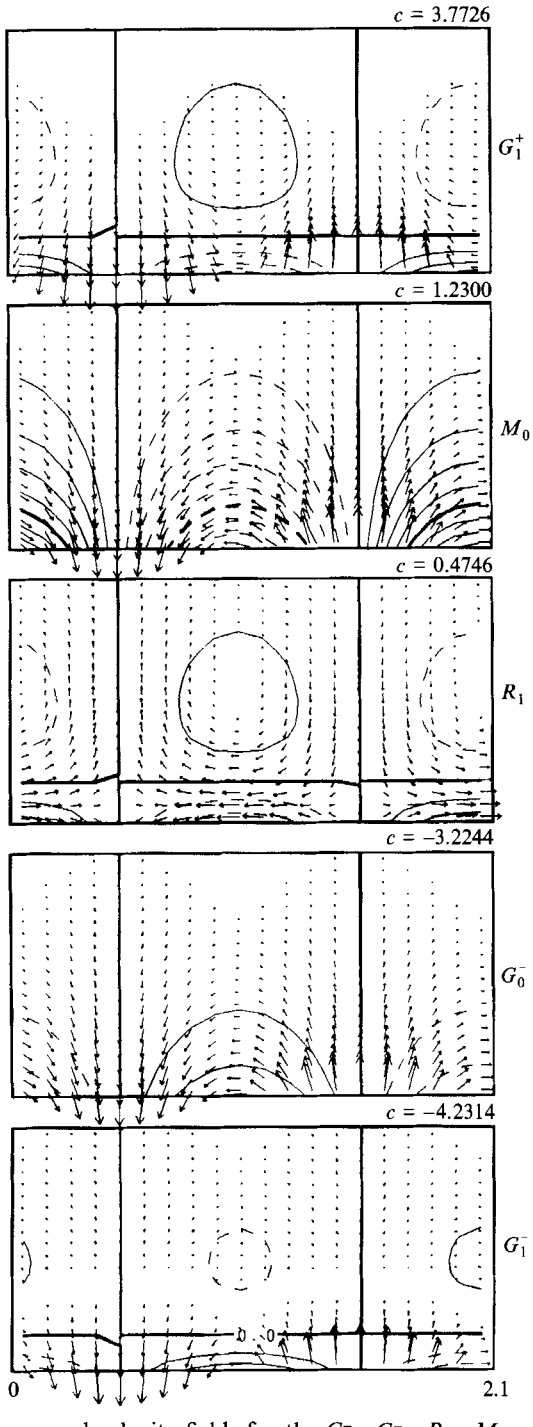

FIGURE 10. Pressure and velocity fields for the G_1^--, G_0^--, R_1-, M_0- and G_1^+-modes, respectively, for $Ri = 3.0$, $Ro = 0.5$.

Figure 9 shows the relation between Ro and c, which can be easily compared to figure 6. Figure 10 shows the structures of modes G_1^-, G_0^-, R_1, M_0 and G_1^+, for $Ri = 3.0$, $Ro = 0.5$.

5. Explanation of the unstable modes

The dashed lines in figures 4, 5 and 6 show the Doppler-shifted dispersion curves of the neutral waves in the one-layer problem for the same Ri. (The dashed curves in figure 6, for example, can be obtained by shifting the curves in figure 9 by $c = 1$.)

First, one can easily see that the bundles of dispersion curves around $c = \pm 1$ correspond to the Rossby modes in each layer. There are many Rossby waves almost trapped in the lower layer, whose intrinsic phase speeds are very small, and their Doppler-shifted phase speeds become almost -1. In the same way, the Doppler-shifted phase speeds of the Rossby waves almost trapped in the upper layer are almost equal to 1.

By comparing the dispersion curves in the two-layer problem and those in the reduced one-layer problem, these figures make it clear which neutral waves resonate to cause each unstable mode. The unstable modes found in figure 3 are schematically classified in figure 11.

The unstable mode named (R) by Orlanski (1968) is caused by a resonance between two M_0-modes (the mixed mode of a Rossby wave and an inertial gravity wave), and the (E)-mode is caused by two R_1-modes (the first Rossby mode). This classification of the (E)-mode is consistent with the result by Orlanski (1968) that the (E)-mode is a baroclinic instability, because Sakai (1989) showed that baroclinic instability is caused by a resonance between two Rossby waves. The mode (E) is, however, somewhat influenced by the interaction of M_0 rather than caused purely by a resonance between two R_1-modes, since there exists an (R)-mode caused by a resonance between two M_0-modes in the vicinity of $c \sim 0$ where the R_1-modes resonate. In the same way, the unstable modes caused by a resonance between two $R_n (n \geqslant 2)$ modes (according to Orlanski 1968, these modes exist at $Ri \geqslant n(n+1)$) are also influenced by the interaction between R_m-modes ($m < n$) and M_0, although these new unstable modes do not appear in the region of $Ri < 3.0$ shown here.

Various kinds of unstable modes exist in the (H)-region; some of them are Rossby–gravity instability caused by resonance between a G_n-mode and R-modes, and another is caused by a resonance between the G_1-mode and the M_0-mode. As stated in the previous section, the M_0-wave behaves like an inertial gravity wave for $Ro > 1$. Hence, this unstable mode caused by a resonance between the G_1-mode and the M_0-mode at large R_0, can be considered to be caused by a resonance between two inertial gravity waves (the first mode and the zeroth mode). Since Sakai (1989) showed that Kelvin–Helmholtz instability is caused by a resonance between two gravity waves, this mode can be regarded as a kind of Kelvin–Helmholtz instability. Orlanski (1968) investigated only a few cases in this (H)-region. He mainly investigated for the points on the line of $Ro = 3.0$, where this M_0–G_1-mode does in fact spread, and seems to have imagined that this unstable mode spread over the whole (H)-region, thus concluding by mistake that the (H)-region corresponded to Kelvin–Helmholtz instability.

The unstable mode, called (B) by Orlanski (1968) and suggested to be Rossby–Kelvin instability by Sakai (1989), is caused by a resonance between R_1 (a Rossby wave) and M_0 (the mixed mode of a Rossby wave and an inertial gravity wave). Consequently, whether this suggestion is right depends on whether the M_0-mode is a Kelvin wave. In the strictest sense, it is a necessary condition of a Kelvin wave that the velocity

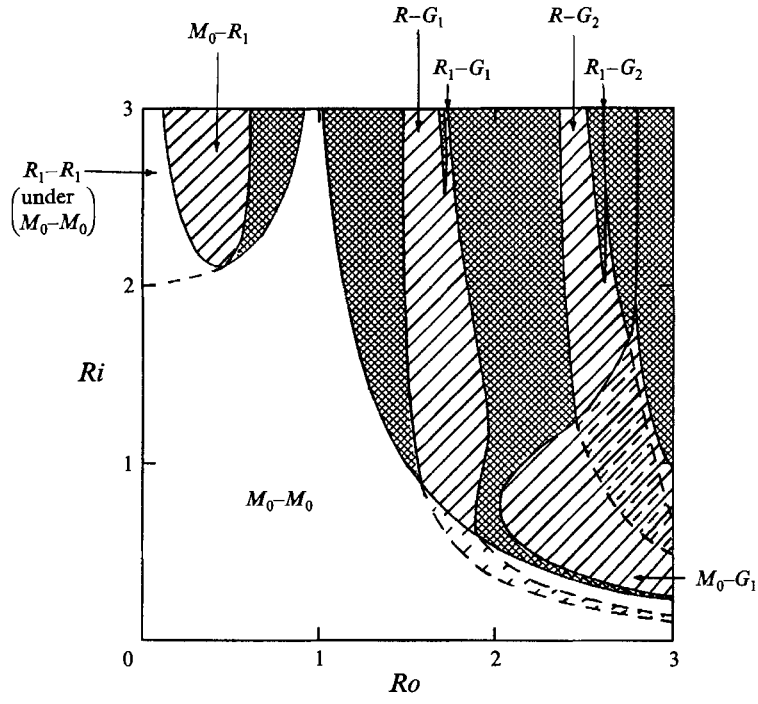

FIGURE 11. The classification of the obtained unstable modes. M_0–R_1, for example, indicates that the unstable mode is caused by a resonance between M_0-mode and R_1-mode. There is no unstable mode in the cross-hatched regions. The unstable modes in the hatched areas have complex eigenvalues. Dashed lines indicate that there are other unstable modes over that one.

component vertical to the boundary of the fluid vanishes. In a limited sense, if not so strict, such a wave is called a Kelvin wave if it possesses features of a gravity wave along the boundary (hence in the direction of propagation), and is almost balanced geostrophically in the direction vertical to the boundary. On the other hand, in a general sense, a wave that is the fundamental mode mixed with a Rossby wave and an inertial gravity wave in a certain system, could be called a 'generalized Kelvin wave'. In this general sense, the M_0-mode is nothing other than a generalized Kelvin wave, and accordingly the (B)-mode can be called Rossby–Kelvin instability. Nevertheless, Sakai (1989) seems to have thought of the Kelvin wave in the limited sense, and to have regarded it as a kind of gravity wave, particularly noticing the features in the direction of propagation, since he expressed Rossby–Kelvin instability as 'an instability caused by a resonance between Rossby waves and gravity waves'. In this limited sense, it is not appropriate to call the M_0-mode a Kelvin wave, because it depends not on the direction but on the value of Ro, whether this mode maintains a geostrophic balance or not. Since an unstable mode (B) is located in the region $Ro < 1$, the resonating M_0-wave has features of a Rossby wave rather than an inertial gravity wave. Hence, the (B)-mode should be considered as a geostrophic instability caused by a resonance between the zeroth and the first Rossby modes, rather than between a Rossby wave and a gravity wave as suggested by Sakai (1989). Figure 12 illustrates the structure of the unstable mode (B). Comparing this figure with figure 10, it can be easily understood that M_0 and R_1 resonate to cause the (B)-mode.

The limiting case of $Ri = 0$ demands special consideration. Orlanski (1968) gave special treatment to this case: this problem is no longer a two-layer problem but is

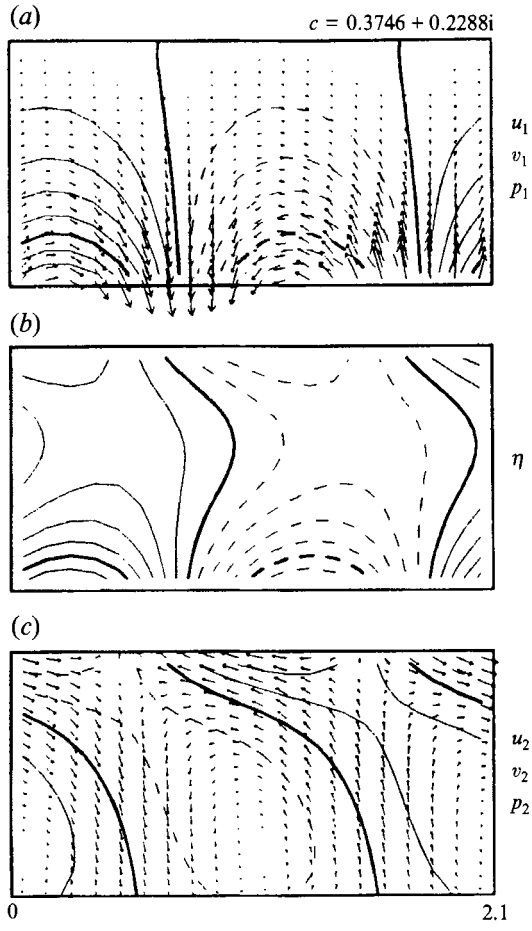

FIGURE 12. The structure of the unstable (B)-mode ($Ri = 3.0, Ro = 0.5$): (*a*) pressure and velocity fields of the first (lower) layer, and (*c*) of the second (upper) layer. Interface height is shown in (*b*). The field of the first layer is like that of the M_0-mode and the second layer of the R_1-mode.

substantially a one-layer problem. Accordingly, this case cannot be described by the interaction between the modes in the reduced one-layer subsystems. However, this case is the problem of Rayleigh-shear instability and this instability can be interpreted as a horizontal interaction between two Rossby waves (vorticity waves) in the entire single layer (e.g. Hayashi & Young 1987; Sakai 1989).

We have often used the term 'a resonance of waves'. This idea can be understood in detail by using the concepts of 'difference energy E' or 'difference momentum M' (e.g. Cairns 1979; Hayashi & Young 1987; Sakai 1989).† The difference energy is defined as the energy in the fluid where waves are excited minus that in the undisturbed fluid where waves are not excited. A mode with non-zero difference energy must be neutral. That is because, if such a mode is amplified, the energy of the whole system must be changed, and such a wave cannot be excited owing to the conservation of energy, as long as there are no external forces. Thus, the difference energy of an

† They used the terms of 'wave energy' or 'disturbance energy' instead of 'difference energy'. However, these terms are often used with a different meaning, and are confusing.

unstable mode must vanish. This leads to the important conclusion that two waves must have difference energies of opposite signs to resonate and form an unstable mode. The difference momentum is similarly defined and similar conclusions can be reached: two neutral waves which resonate to cause an unstable mode have difference momenta of opposite signs and the difference momentum of the unstable mode vanishes. These two criteria expressed by difference energy, E, and difference momentum, M, are equivalent, because of the simple relation $E = cM$ between these two quantities. Particularly for two-layer problems, it was shown by Sakai (1989) that the difference momentum has the same sign as that of the intrinsic phase speed of the waves (the phase speed relative to the basic flow).

This idea is applied to the problem considered here. Although there is no strong reason to choose either the difference energy or the difference momentum, whose analyses are equivalent, the difference momenta are calculated here, because the value of the difference energy depends on the frame of reference, while that of the difference momentum does not (Sakai 1989). The difference momentum is expressed as follows in dimensional units (see equation (2.31) in Hayashi & Young 1987 or (5) in Sakai 1989):

$$M_* = M_{R*} + M_{G*}, \tag{77}$$

where

$$M_{R*} \equiv -\frac{1}{2}\left\langle \bar{\eta}_*^2 \frac{\mathrm{d}Q_{1*}}{\mathrm{d}y_*} \xi_{1*}'^2 \right\rangle - \frac{1}{2}\left\langle (H-\bar{\eta}_*)^2 \frac{\mathrm{d}Q_{2*}}{\mathrm{d}y_*} \xi_{2*}'^2 \right\rangle, \tag{78}$$

$$M_{G*} \equiv \langle \eta_* u_{1*}' \rangle - \langle \eta_* u_{2*}' \rangle, \tag{79}$$

where ξ_j' are the particle displacements in the y_*-direction, $Q_{1*} \equiv f/\bar{\eta}_*$ and $Q_{2*} \equiv f/(H-\bar{\eta}_*)$ are the potential vorticities of the basic state, and the angle brackets denote the spatial integral. Non-dimensionalizing M_* by $M_* \equiv (H\Delta U/2)M$, these equations become

$$M = M_R + M_G, \tag{80}$$

where

$$M_R \equiv \frac{1}{4Ri\,Ro^2}\left(\left\langle \frac{v_1^2}{(c+1)^2} \right\rangle - \left\langle \frac{v_2^2}{(c-1)^2} \right\rangle\right), \tag{81}$$

$$M_G \equiv \langle \eta u_1 \rangle - \langle \eta u_2 \rangle. \tag{82}$$

The values of these difference momenta are plotted in figure 13. Each unstable mode, which itself has the difference momentum of zero, is formed by the interaction between a mode with positive difference momentum and a mode with negative difference momentum.

Figure 14, which shows a broader range than figure 4, illustrates simultaneously the dispersion curves of two-layer and one-layer problems. In the region $|c_r| > 1$, there are several intersections of G_n^+-modes and G_m^--modes for the one-layer problem, which does not cause unstable modes for the two-layer problem. This is explained as follows: G^+-mode in the first layer and a G^--mode in the second, or vice versa, have intrinsic phase speeds of the same sign, and they do not resonate even if they intersect. Furthermore, two G^--modes or an R and a G^- never intersect. Consequently, although there are six combinations of waves in the first and second layers (regarding M_0 as R or G^+), only three combinations of R–R, G^+–G^+ and R–G^+ resonate to cause unstable modes in reality. That is why the plusses of the G_n^+-modes are eliminated in the names of unstable modes.

Some analytical results of Kotschin (1932) and Orlanski (1932) can be interpreted as features of the waves in the reduced one-layer system, by using this idea of the resonance of waves. Kotschin (1932) showed that the curve indicating $c = 0$ has a singularity at $Ro = 0$, which can be explained as follows: as was shown in §4, the value

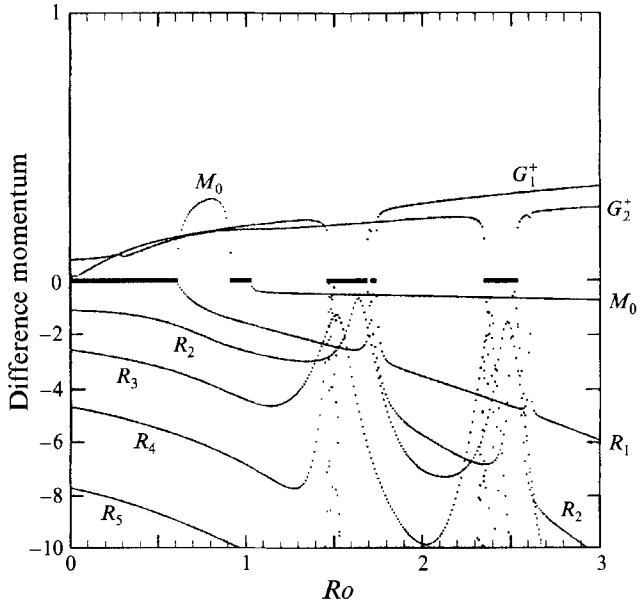

FIGURE 13. Difference momentum for the waves with positive phase speed at $Ri = 3.0$. The difference momenta of higher gravity modes are eliminated. Unstable modes are shown by thick lines. All the unstable modes have the difference momenta of zero. The difference momenta are normalized by wave amplitude ($\langle y(u_1^2+v_1^2)+(1-y)(u_2^2+v_2^2)+4Ri\,\eta^2\rangle$). The scale for positive momenta is multiplied by 10.

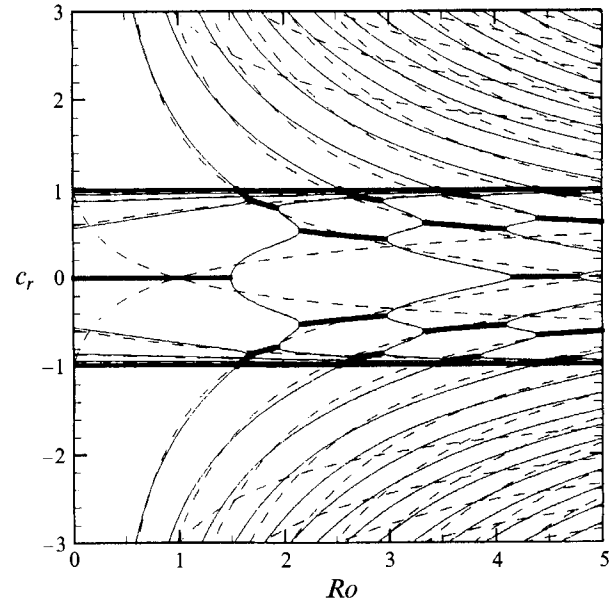

FIGURE 14. c_r as a function of Ro at $Ri = 1.0$. A broader region than in figure 4 is shown. There are some intersections of G^+ and G^- which do not resonate to cause unstable modes in the region of $|c_r| > 1$.

of c for the M_0-mode always becomes 1 at $Ro = 1$, whatever the value of Ri. For the two-layer problem, consequently, the Doppler-shifted phase speeds of the M_0-modes vanish in both layers, and resonate to cause the (R)-mode (figure 15).

Equation (76) shows that the value of Ri at which the value of c for the nth Rossby

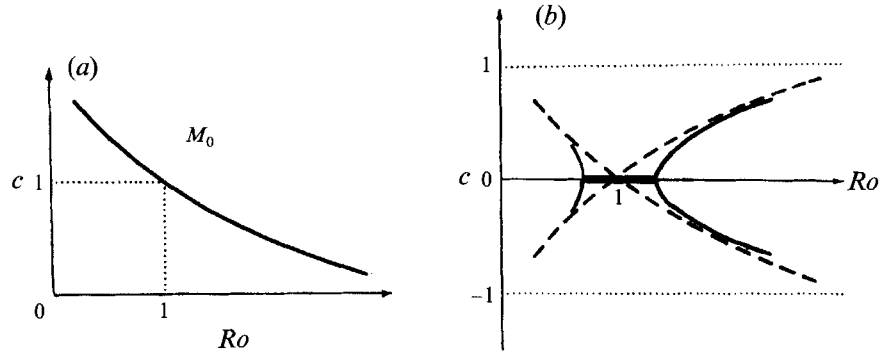

FIGURE 15. Explanation of the singularity which the curve of $c = 0$ has at $Ro = 1$. (*a*) For the one-layer problem, the value of c for the M_0-mode becomes 1 at $Ro = 1$, whatever the value of Ri. (*b*) Dashed lines indicate Doppler-shifted dispersion curves for the one-layer problem, and the solid lines dispersion curves for the two-layer problem. Doppler-shifted M_0-modes of the both layers intersect at $Ro = 1, c = 0$, and resonate to cause an unstable mode.

mode with very long wavelength becomes 1 is almost proportional to n^2. Since waves with phase speed $c = 1$ in the one-layer model are Doppler-shifted to resonate in the two-layer model, this corresponds to the result by Orlanski (1968) that a new unstable mode appears at $Ri = n(n+1)$, which is also almost proportional to n^2. There is a difference between the coefficients of the n^2, which is because the waves begin to resonate before their Doppler-shifted phase speeds coincide completely.

Finally, let us see which unstable mode grows fastest for each value of Ri. The largest growth rate is associated with the M_0–R_1-mode if $Ri > 2.3$, and with the M_0–M_0-mode if $1.0 < Ri < 2.3$. On the other hand, if $Ri < 1.0$, unstable modes with large Ro caused by resonances between two higher G-modes have largest growth rates. Therefore, in this frontal system, geostrophic instability dominates if $Ri > 1.0$, while Kelvin–Helmholtz instability with small scale dominates if $Ri < 1.0$.

6. Conclusions

The stability of the front model treated by Orlanski (1968) is re-examined using a matrix method, by which one can obtain all of the eigenvalues directly. Also, the features of the neutral waves in the reduced one-layer problem are investigated, and the results are summarized as follows:

(i) The unstable modes called (H) and (B) were not described correctly by Orlanski (1968). Unstable modes do not cover the entire (Ri, Ro)-plane.

(ii) The unstable modes studied by Orlanski (1968), and partly corrected in this paper, are classified by identifying which waves resonate to cause the instability. The unstable mode called (B) by Orlanski (1968), and suggested by Sakai (1989) to be a Rossby–Kelvin instability caused by a resonance between a Rossby wave and a gravity wave, is a geostrophic instability caused by a resonance between mode M_0 (the mixed mode of a Rossby wave and a gravity wave) with long wavelength (accordingly, having features of a Rossby wave) and mode R_1 (the first Rossby mode).

(iii) Some analytical characteristics of this problem, such as the singularity at $Ro = 1$ of the curve for $c = 0$, and the appearance of new unstable modes, are explained by the features of the neutral waves in the one-layer problem using the idea of resonance.

(iv) The largest growth rate is associated with a geostrophic unstable mode if $Ri > 1.0$, and with Kelvin–Helmholtz instability with small scale if $Ri < 1.0$.

The author thanks Professor T. Asai and R. Kimura for their useful suggestions and encouragement. He also would like to express thanks to Dr Y.-Y. Hayashi and Mr S. Takehiro for their fruitful discussions. He is grateful to Dr J. Whitehead for reading the manuscript and giving valuable comments. The IMSL Library was used for solving the eigenvalue problems and the NCARG Library was used for drawing the figures.

Appendix A. Numerical calculations by finite differences

For the two-layer problem, the variables u_j, v_j, ζ_j, D_j and FD_j are located as shown in figure 16. ζ_j, D_j and FD_j are calculated from u_j and v_j as follows ($\Delta y \equiv 1/N$):

$$\zeta_{j(l-\frac{1}{2})} = 2\mathrm{i}Ri\,Ro\,v_{j(l-\frac{1}{2})} - (1/\Delta y)(u_{j(l)} - u_{j(l-1)}), \tag{A 1}$$

$$D_{j(l)} = (1/\Delta y)(v_{j(l+\frac{1}{2})} - v_{j(l-\frac{1}{2})}) + 2\mathrm{i}Ri\,Ro\,u_{j(l)}, \tag{A 2}$$

$$FD_{j(l)} = (1/\Delta y)(y_{j(l+\frac{1}{2})}\,v_{j(l+\frac{1}{2})} - y_{j(l-\frac{1}{2})}\,v_{j(l-\frac{1}{2})}) + 2\mathrm{i}Ri\,Ro\,y_{j(l)}\,u_{j(l)}, \tag{A 3}$$

where

$$y_{1(l)} \equiv l/N, \quad y_{2(l)} \equiv (N-l)/N.$$

By using these variables, (38)–(41) are finite differenced as follows:

$$\mathrm{i}Ro\,c\zeta_{1(l-\frac{1}{2})} = -\mathrm{i}Ro\,\zeta_{1(l-\frac{1}{2})} + (1/2y_{1(l-\frac{1}{2})})(y_{1(l-1)}\,D_{1(l-1)} + y_{1(l)}\,D_{1(l)}), \tag{A 4}$$

$$\mathrm{i}Ro\,c\zeta_{2(l-\frac{1}{2})} = \mathrm{i}Ro\,\zeta_{2(l-\frac{1}{2})} + (1/2y_{2(l-\frac{1}{2})})(y_{2(l-1)}\,D_{2(l-1)} + y_{2(l)}\,D_{2(l)}), \tag{A 5}$$

$$c(FD_{1(l)} + FD_{2(l)}) = FD_{1(l)} - FD_{2(l)}, \tag{A 6}$$

$$\mathrm{i}Ro\,c(u_{1(l)} - u_{2(l)}) = \mathrm{i}Ro(u_{1(l)} + u_{2(l)}) + y_{1(l)}\,D_{1(l)} + y_{2(l)}\,D_{2(l)}. \tag{A 7}$$

For the one-layer problem, the variables u, v and η are located as shown in figure 16, and $y_{(l)}$ is defined as

$$y_{(l)} \equiv l/N.$$

Equations (42)–(44) are finite differenced as follows:

$$\mathrm{i}Ro\,cu_{(l)} = -\tfrac{1}{2}(v_{(l+\frac{1}{2})} + v_{(l-\frac{1}{2})}) + 4\mathrm{i}Ri\,Ro\,\eta_{(l)}, \tag{A 8}$$

$$\mathrm{i}Ro\,cv_{(l-\frac{1}{2})} = (1/2y_{(l-\frac{1}{2})})(y_{(l)}\,u_{(l)} + y_{(l-1)}\,u_{(l-1)}) + (2/\Delta y)(\eta_{(l)} - \eta_{(l-1)}), \tag{A 9}$$

$$\mathrm{i}Ro\,c\eta_{(l)} = \mathrm{i}Ro\,y_{(l)}\,u_{(l)} + (1/2Ri\,\Delta y)(y_{(l+\frac{1}{2})}\,v_{(l+\frac{1}{2})} - y_{(l-\frac{1}{2})}\,v_{(l-\frac{1}{2})}). \tag{A 10}$$

For both the one-layer and two-layer problems, most computations were done with $N = 20$. The results were tested with $N = 40$ at some parameters. There was no important difference between results with $N = 20$ and those with $N = 40$.

Appendix B. Laguerre functions

The regular solution at $z = 0$ of the differential equation

$$z\,\mathrm{d}^2u/\mathrm{d}z^2 + (1-z)\,\mathrm{d}u/\mathrm{d}z + \nu u = 0 \tag{B 1}$$

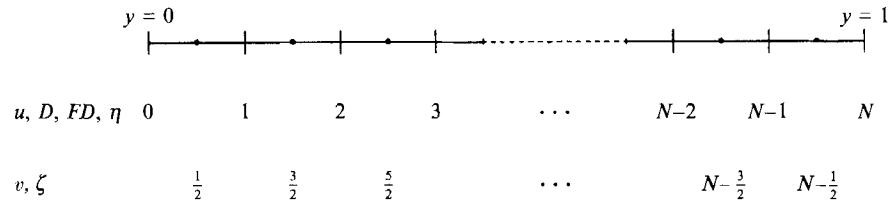

FIGURE 16. Location of the variables.

is Laguerre function of zeroth order,

$$u = L_\nu^{(0)}(z) = F(-\nu, 1; z) = \sum_{n=0}^{\infty} \frac{(-\nu)_n z^n}{(n!)^2}, \tag{B 2}$$

where $$(\beta)_n \equiv \beta(\beta+1)\dots(\beta+n-1).$$

As is evident from its definition, for $\nu = 0, 1, 2, \dots$, the function $L_\nu^{(0)}(z)$ becomes a polynomial with finite terms and is called Laguerre polynomial.

Differentiating this function $L_\nu^{(0)}(z)$, we obtain

$$\frac{\mathrm{d}}{\mathrm{d}z} L_\nu^{(0)}(z) = \frac{\mathrm{d}}{\mathrm{d}z} \sum_{n=1}^{\infty} \frac{(-\nu)_n z^n}{(n!)^2} = \sum_{n=1}^{\infty} \frac{(-\nu)_n z^{n-1}}{n!(n-1)!}. \tag{B 3}$$

If $\nu < 0, z > 0$, all the summed terms are positive, and the value of $\mathrm{d}L_\nu^{(0)}(z)/\mathrm{d}z$ never vanishes.

In the case of $\nu = n+\epsilon (n = \text{integer}, 0 < \epsilon \ll 1)$, $L_\nu^{(0)}(z)$ almost equals to the polynomial of nth order $L_n^{(0)}(z)$ within the range of moderate value of z, but as z grows to infinity, the absolute value of $L_\nu^{(0)}(z)$ grows exponentially with sign opposite to that of the coefficient of the highest term of $L_n^{(0)}(z)$. Since all the terms higher than nth order include the small coefficient $(-\epsilon)$, as ϵ approaches zero, the largest extreme point goes to infinity. Therefore, when finding the ν that makes $z = z_0$ the extreme point of $L_\nu^{(0)}(z)$, ν approaches n, as z_0 grows to infinity.

REFERENCES

CAIRNS, R. A. 1979 The role of negative energy waves in some instabilities of parallel flows. *J. Fluid Mech.* **92**, 1–14.

HAYASHI, Y.-Y. & YOUNG, W. R. 1987 Stable and unstable shear modes on rotating parallel flows in shallow water. *J. Fluid Mech.* **184**, 477–504.

KOTSCHIN, N. 1932 Über die Stabilität von Margulesschen Diskontinuitätsflächen. *Beitr. Phys. Atmos.* **18**, 129–164.

MYSAK, L. A. 1968 Edgewaves on a gently sloping continental shelf of finite width. *J. Mar. Res.* **26**, 24–33.

NAKAMURA, N. 1988 Scale selection of baroclinic instability – effects of stratification and nongeostrophy. *J. Atmos. Sci.* **45**, 3253–3267.

ORLANSKI, I. 1968 Instability of frontal waves. *J. Atmos. Sci.* **25**, 178–200.

REID, R. O. 1958 Effect of Coriolis force on edge waves. (I) Investigation of the normal modes. *J. Mar. Res.* **16**, 109–144.

ROBINSON, A. R. 1964 Continental shelf waves and the response of sea level to weather systems. *J. Geophys. Res.* **69**, 367–368.

SAKAI, S. 1989 Rossby–Kelvin instability: a new type of ageostrophic instability caused by a resonance between Rossby waves and gravity waves. *J. Fluid Mech.* **202**, 149–176.

SATOMURA, T. 1981 An investigation of shear instability in a shallow water. *J. Met. Soc. Japan* **59**, 148–167.